ISOLDE: ISS-BASED STUDY OF LEO DEBRIS AND METEOROID ELECTRICAL EFFECTS

Ivan Linscott[1], Sigrid Close[1], Ashish Goel[1], Nicolas Lee[1], Stan Green[2], Nevin Bryant[3]

[1]*Stanford University, 264 Durand Bldg, Stanford University, Stanford CA 94305, sigridc@stanford.edu*
[2]*Individual Contributor, 6456 Wishbone Terrace, Cabin John, MD20818 green6456@verizon.net*
[3]*Jet Propulsion Laboratory, 4800 Oak Grove Drive, Pasadena, CA,nevin.a.bryant104338@jpl.nasa.gov*

Abstract

The International Space Station (ISS), presents a unique platform for performing hypervelocity impact experiments. Using for example the MISSE-X format, a new container design for experiments fixed on the ISS exterior, a suite of instrumentation can be accommodated to observe a combination of optical flash, plasma production, particle detection and electromagnetic (EM), radiation from a hypervelocity impact of nano-gram and larger particles. The impact surface available in the MISSE-X format is ~1 m^2, sufficient to intercept incident flux at rates that afford excellent statistical surveys of nano to microscale particles.

1 Science Objectives and Measurements

The objective of the ISS-based Study Of LEO Debris and meteoroid Electrical effects (ISOLDE) mission is to provide the first characterization of hypervelocity impact plasma stemming from meteoroid collisions with spacecraft. ISOLDE will host sensors on an ISS payload platform designed to characterize the plasma and associated radio frequency (RF) emission and give the first link to measurements from ground-based impact experiments. The primary goals are to determine the parameters of small meteoroids that are numerous yet difficult to detect using ground-based instruments, and to provide the first in situ characterization of the resulting plasma that is produced upon impact.

1.1 Background

Meteoroids are a component of space weather that can affect the Earth's ionosphere and influence the performance and reliability of space and ground-borne technological systems. Impacts of meteoroids on spacecraft can produce extremely dense plasmas with dynamics unique to this phenomenon. However, compared to other space weather phenomena like the solar wind, meteoroids remain difficult to study and relatively unknown.

For the purposes here, meteoroids are simply any naturally occurring, solid extraterrestrial object smaller than 1 m with no lower limit on size. The vast majority of detected meteoroids originate from comet and asteroid debris streams within our Solar System, while a small percentage (< 3%) have an interstellar origin. Sporadic meteoroids primarily originate from six apparent sources relative to the Earth (Fig. 1), including the North and South Apex, North and South Toroidal, Helion and Antihelion, and lesser-known Asteroidal source [1]. Shower meteoroids, which occur at a specific time each year, are associated with a particular comet or asteroid. Meteoroid studies have been undertaken using ground-based observations and in situ detection methods.

Figure 1. Geometry of sporadic meteor sources.

Meteoroid parameters, such as mass and density, are inferred from ground based radar measurements through plasma modeling efforts [2], subject to errors and uncertainties introduced through the modeling process. The meteoroid input flux determined from these measurements is roughly 20 to 40 Tonnes/day, although highly uncertain because of the detection limits of the radar facilities. Particles with mass less than 1 μg are expected to have a very large presence in the atmosphere [3].

Meteoroids upon impact, they produce a dense plasma; the amount of charge produced is dependent on the mass and speed of the meteoroid. Empirical studies have established a power law dependence of the form

$$q = 0.1m\left(\frac{m}{10^{-11}}\right)^{0.02}\left(\frac{v}{5}\right)^{3.48} \qquad (1)$$

Proc. '6th European Conference on Space Debris'
Darmstadt, Germany, 22–25 April 2013 (ESA SP-723, August 2013)

where q is the total charge in Coulombs, m is the meteoroid mass in grams, and v is the impact speed in km/s [4]. The strong dependence on speed is significant because meteoroids can travel at up to 72.8 km/s relative to the Earth, greater if they are of interstellar origin. In situ measurements of meteoroids by spacecraft have exploited this effect to detect charge formation from impacts of meteoroids on a collecting surface. In situ sensors have flown on Pioneer 8 and 9, Hiten, Galileo, Ulysses, Cassini, Helios and NOZOMI [5][6][7]. Space-based in situ impact detectors can detect meteoroids with mass less than 1 μg.

Studies of impact plasmas have been performed at ground-based facilities including Van de Graaff dust accelerators, light gas guns, and plasma drag accelerators. However, there is no technology that fully replicates the projectile masses and speeds associated with meteoroid impact. Additionally, the ambient pressure achievable at most light gas gun facilities is on the order of 0.1 mbar. This corresponds to a mean free path of millimeters, resulting in a collisional expansion of the impact plasma into the ambient atmosphere. The effect of ambient atmosphere has been studied for expanding plasma plumes from laser ablation studies [8] and is significant for impact plasmas as well. Even with Van de Graaff dust accelerators, where the vacuum levels are typically on the order of 10^{-6} mbar, the size of the test chamber itself becomes the limitation, with reflected signals manifesting within nanoseconds of the impact event.

As a result of these many challenges, there has been no complete analysis of the phenomenon of electromagnetic emission from hypervelocity impact. Instead, there remains much disagreement in the field about the mechanisms behind impact-induced radiation. Reference [9] attribute impact light flashes to rapid recombination of a fully-ionized plasma, while [10] conclude that light flashes are not due to recombination since they are not affected by direct plasma measurements, which inhibit recombination. [11] associate their detected microwave signals to microcracking, while [12][13] posit a macroscopic charge separation, which may be due to their use of a powdered dolomite target rather than the more commonly studied solid metallic targets.

1.2 ISOLDE Science Objectives

ISOLDE will provide the first in situ understanding of the processes associated with meteoroid impact plasmas, as well as a characterization of the small meteoroids, which is difficult to achieve using only ground-based sensors. ISOLDE will achieve the following three science objectives:

1) Investigate the properties of the plasma generated from a meteoroid impact: The specific focus will be on plasma formation, including charge production, plasma density, expansion speed, energy distribution and temperature.
2) Investigate the emission of RF radiation from impact-induced plasma: Determine the radiated power as a function of frequency and correlate with ground-based impact measurements. Probe the fundamental physics responsible for emission of radiation from plasmas to understand the mechanism by which this radiation couples to satellite electronic systems.
3) Improve knowledge and understanding of small meteoroids in earth's space environment: Low-mass (10^{-15} g to 10^{-6} g) meteoroids are difficult to detect using ground-based facilities because of the associated low plasma density formed upon its ablation in the atmosphere.

1.3 Meteoroid Impact Plasma Characterization: Supporting Research

When a meteoroid impacts a satellite, both the meteoroid as well as a fraction of the target is vaporized and ionized, forming a dense plasma cloud. The subsequent expansion is not yet well characterized. Stanford University has undertaken theoretical, computational and experimental efforts in order to better understand this phenomenon.

Theoretical

A theoretical model was developed to explain the mechanism behind the generation of impact plasma [14]. Upon impact, the electrons, with lower masses and hence larger thermal velocities, expand first, followed by the slower ions. This charge separation sets up an ambipolar electric field that results in a coherently oscillating electron population expanding with the ion into the surrounding vacuum at the isothermal sound speed, which is typically 10s of km/s. Fig. 2 depicts this expansion process (left panel) and the associated radiated power (right panel).

Computational

The computational simulation extends the theoretical interpretation of the meteoroid impact plasma and is divided into two phases. First, a hydrocode is used to simulate the impact, which includes the shock formation in the meteoroid and satellite material and the plasma formation process. This plasma formation and initial expansion occurs over a period of approximately 10 nanoseconds, producing multiple ion charge states and temperatures on the order of 10 eV.

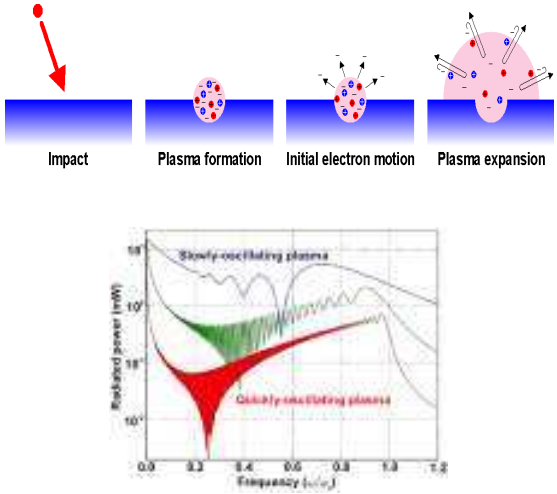

Figure 2. Illustration of the meteoroid impact process, and power.

The plasma expansion is computed using an electromagnetic particle in cell (PIC) code to investigate possible radiation mechanisms in this plasma as it expands into the surrounding vacuum. Example results are shown in Fig. 3. [15] The impact point is centered at the very bottom of the domain, and the plasma is expanding upwards. The radiated frequency (RF) emission occurs at the plasma frequency and decreases as the plasma expands and the density decreases, which is consistent with the theoretical model.

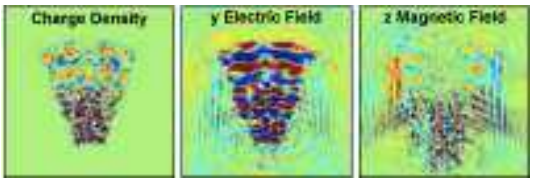

Figure 3. Numerical particle in cell (PIC) simulations of RF emission from impact plasma.

Experimental

Ground-based meteoroid impact tests were conducted at the Van de Graaff dust accelerator facility in the Max Planck Institute for Nuclear Physics (MPIK), Heidelberg, Germany in December 2010 and August 2011 [16][17] images of the experiment are shown in Fig. 4. Spherical iron projectiles with masses ranging from 10^{-11} to 10^{-15} g, similar in composition to naturally occurring meteoroids, were shot at a variety of target surfaces at speeds ranging from 2 to 70 km/s. While the speeds were representative of meteoroids, the masses were up to 10 orders of magnitude smaller than what is usually detected from ground-based radar. The targets were bare metal (tungsten, aluminum, brass, and copper) and spacecraft material samples (solar cells, solar panels and optical surface reflectors) and were set to bias voltages ranging from ground to ±1 kV to simulate surface charging in space.

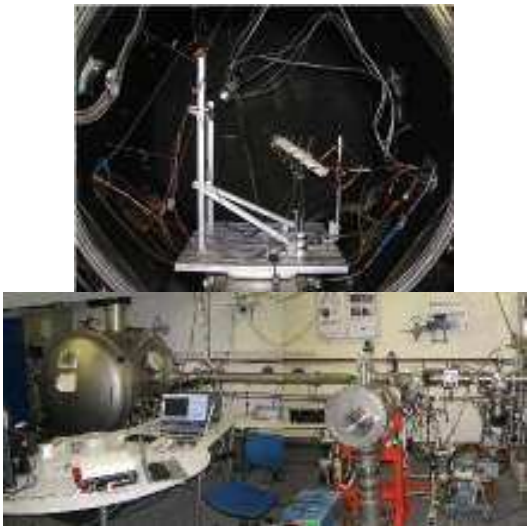

Figure 4. (left) An experimental configuration of various sensors;
(right) The hypervelocity impact test facility at MPIK, Germany.

In order to study the characteristics of the impact plasma and the associated electromagnetic radiation, simultaneous measurements were made with four different sensor suites during the ground-based experiments, including 1) a Photomultiplier Tube (PMT), 2) 2 Retarding Potential Analyzers (RPA), 3) 6 patch antennas (PA) at 315 and 916 MHz, and 4) 2 E-field sensors (SRI). Plasma and associated RF emission was detected from impacts by particles as small as 10^{-15} g. While previous experiments have shown RF emission associated with large impacts on solid surfaces [18], this is the first experiment to demonstrate RF associated with the expanding plasma [19]. Fig. 5 shows an impact event with a corroborative measurement of particle impact, and plasma and RF production.

While the theoretical, computational and ground-based experiment results have provided remarkable insight into this phenomenon, the cannot fully reproduce the satellite conditions, background atmospheric and ionospheric conditions, and most importantly the conditions of the meteoroid population through this approach. Hence results from space are necessary to gain a complete understanding of the physics behind meteoroid impact plasma.

1.4 ISOLDE Science Measurements and Requirements

In order to meet the science objectives listed above, the ISOLDE instrument package will have designated impact surfaces covered with a thin sheet of tungsten target material. Three types of sensors will be utilized to characterize the impacts on the surfaces, including 1) optical sensors, 2) plasma

sensors, and 3) RF sensors. The optical sensors will measure the intensity of the impact flash and its time evolution, enabling us to determine the time of impact and calculate the

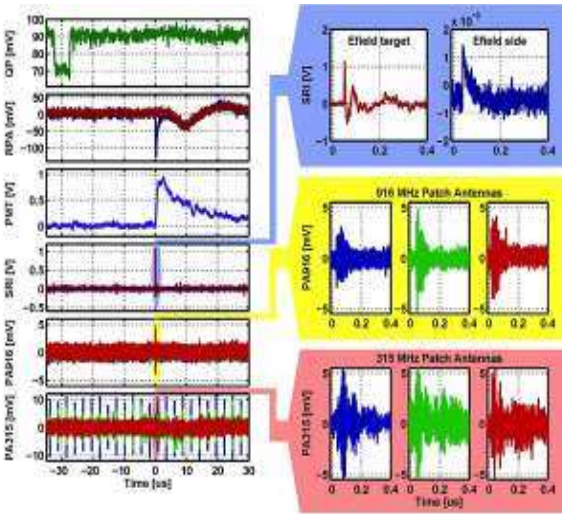

Figure 5. Multi-sensor response to meteoroid impact on a tungsten target. On the left from top to bottom, Q-pulse indicating mass and speed of projectile, RPA response, PMT response, E-field (SRI) signal, 916 MHz and 315 MHz patch antenna signal waveforms.

location of impact. The optical measurements will also provide the flux of meteoroids, and combined with information about the attitude of the satellite, and determine the radiant direction of the impacting meteoroids. The plasma sensors will measure the ion and electron number densities and their time evolution across multiple energy bands, and determine the charge generated, the energy distribution of plasma, the electron and ion temperatures, and the meteoroid composition. The RF sensors will measure the electromagnetic radiation at three different frequencies (150 MHz, 315 MHz, and 916 MHz).

A representation of the instrument package with the optical, plasma, and RF sensors is included in Figure 6.

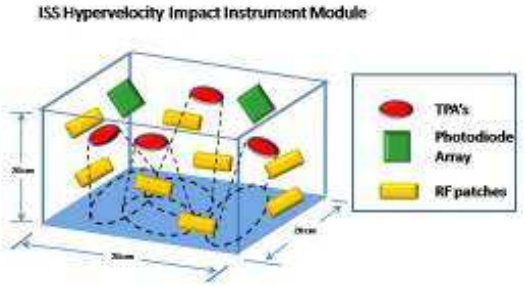

Figure 6. ISOLDE Instrument Package Module. Sensors are included are photomultiplier tubes (PMT's) for optical flash, Transient Plasma Analyzers (TPA's) for plasma, and RF patch antennas to sample the EM radiation over frequencies from 150 MHz to 916 MHz. The sensors are mounted within an open frame package, with a cover that is removed after deployment on the ISS. Multiple modules will be provided for deployment

1.5 ISOLDE Instrumentation Design

The ISOLDE instrument module will consist of a sensor suite to perform optical, plasma, and RF measurements along with a signal processing, data acquisition, and triggering system to achieve the science objectives. The sensor suite proposed is similar to the sensors that were used in the ground-based hypervelocity impact tests described in Section 1.3. The experience of having extensively used similar sensors and amplifying circuits in vacuum environment has been especially valuable in designing this second generation instrumentation.

1.5.1 Instrument Configuration

ISOLDE will house the sensor suite in an open frame cube, 20 cm on each side. The package will be protected by a cover that is removed after attachment to the ISS. Data acquisition for the instrument module is supported by a separate package intended to be contained inside the ISS. The impact surface in the instrument module is the bottom panel, 0.031" thick, covered with a thin sheet of tungsten. The sensors will be mounted for two opposing views of the impact surface. The effective meteoroid impact area on the instrument is approximately 0.04 m^2 per module, with the expectation for deploying 4 to 8 modules, and a total impact area of 0.16 m^2 to 0.32 m^2 . Since the majority of the ground-based impact tests were performed with tungsten target material, the use of tungsten in space wll support the construction of a holistic model of meteoroid impact phenomena by combining ground based and space based data. Fig. 6 depicts the ISOLDE instrument package.

1.5.2 Optical Sensors

An array of 16 photodiodes will be used to detect the strength and time evolution of optical flash from hypervelocity impacts. The photodiodes will also be used to determine the location of impacts on the impact surfaces (camera sensors do not have the sensitivity or speed necessary for measuring weak transient flashes). We will utilize the UDT-4X4D photodiode array from OSI Optoelectronics because of its high response, low capacitance and low Noise Equivalent Power (NEP) (Fig. 7).

A small lens will be mounted on top of the detector array to create a mapping between the source plane (impact surface) and the image plane (detector array). The location of impact can then be

determined with up to 1 cm accuracy by comparing the relative strengths of the intensity measured by the different photodiodes. The velocity of the meteoroid can be derived from the rise time of the optical signal [20]. The strength of the optical and plasma signals varies with the mass and velocity of the meteoroid as a power law (Eq. 1). Having estimated the meteoroid speed, the mass of the meteoroid can then be calculated. The time of incidence of optical and plasma signals will also give us an estimate of the plasma expansion speed.

Active area per cell	1 mm²
Responsivity	0.4 A/W
Capacitance	35 pF
NEP	1e-14 $W/\sqrt{Hz}$

Figure 7. Table with the specifications of the photodiode array, and Image of the sensor.

1.5.3 Plasma Sensors

A planar array of electrostatic analyzer wells, denoted the Transient Plasma Analyzer (TPA), will be designed and fabricated to measure the radially expanding plasma plume. The design of the analyzer is based on the ground-based plasma sensors [17] with a configuration similar to the design described by [21][22]. The TPA will measure electron and ion spectra from 1 to 100 eV in discrete energy channels with up to 100 ns time resolution. Each species will be assigned eight energy channels, with each channel composed of nine electrostatic analyzer wells connected to the same collector and amplifier. This layout is shown in Fig. 8 (left and middle panels) with a 5 cm × 5 cm collecting region exposed to the impact surface. The ion channels will discretize the energy channels differently for each species, depending on the atomic mass of the ion. Each individual aperture in the array will have specific dimensions and fixed bias to provide bandpass energy filtering. The redundant apertures increase the collecting area and will mitigate possible clogging by ejecta. The use of redundant apertures rather than a larger single aperture also limits the magnitude of bias voltages required while keeping an electrically simple configuration, and does not change the data sampling requirements.

The TPA can be broken down into three major components, which can be designed and developed in parallel: a high-voltage source to supply the bias levels; the array of electrostatic apertures; and transimpedance amplifiers to condition the sensor signals. The electrostatic analyzers will be modeled in a 3D physics simulation. Modeling in 2D has been performed in MATLAB, as shown in Fig. 8 (right panel). The development of TPAs for space applications is already funded through NASA Ames.

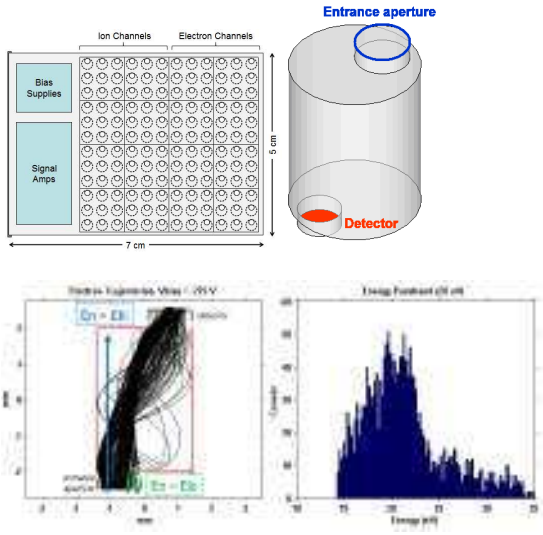

Figure 8. (left) Layout of TPA components; (middle) Geometry of single electrostatic analyzer; (right) Analysis of electrostatic analyzer performance.

By imposing an electrical bias on the impact surface, an electric field is set up between the surface and the plasma sensors. Charges produced by the impact then undergo acceleration inversely proportional to particle mass, allowing the plasma sensor to determine chemical composition of the ion species. In Fig. 9, a plasma measurement from the ground-based experimental campaign at MPIK shows the ion species detected from the impact of an iron particle on tungsten at 35.2 km/s (other elements detected are present as impurities in projectile/target). For approximately 100 impacts, we intend to bias the target surfaces on ISOLDE in order to characterize the meteoroid composition.

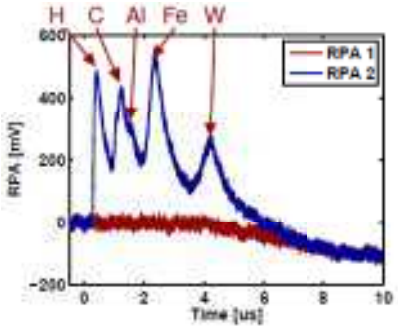

Figure 9. Ion peaks in the waveform measured by the plasma sensor in the MPIK experiments.

1.5.4 RF Sensors

The radio-frequency subsystem is crucial to the detection, quantification, and classification of the plasma-induced emission. As the plasma expands from the impact region, its density decreases,

thereby decreasing the plasma frequency associated with it. Should RF emission arise from the oscillation of sheath electrons at the plasma frequency, radiation should be observed over a spectrum of frequencies as the plasma expands outwards from the point of impact. Hence, in order to probe different phases of the expansion process, patch antennas are chosen as RF sensors at three different frequencies, including 150 MHz, 315 MHz, and 916 MHz, two of which were used in the MPIK experiments. Miniaturized, resonant patch antennas are used to minimize the instrument footprint on ISS. The antennas will have an inherent bandwidth close to 3% of the operating frequency and be circularly polarized. The back-end electronics will comprise low noise amplifiers and data acquisition system. The design and simulated radiation pattern of these antennas is shown in Fig. 10.

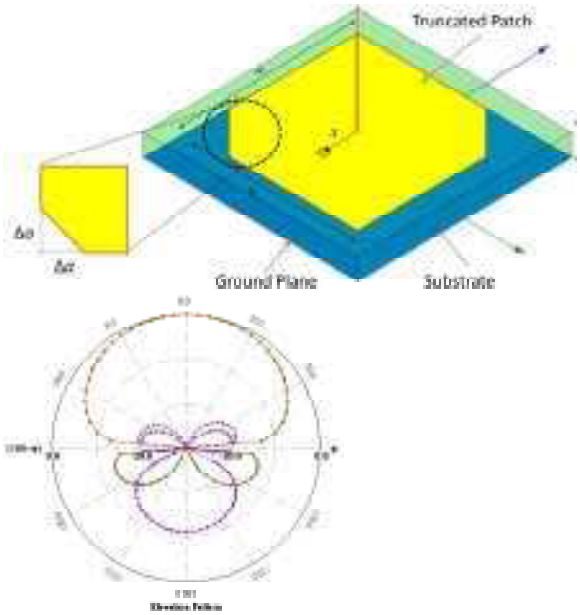

Figure 10. (left) A circularly polarized patch antenna; (right) Radiation pattern of one such antenna.

1.6 Mission Success Criteria

The minimum success criteria for the ISOLDE experiment will be met if data for 400 meteoroid impacts are captured during the lifetime of the mission (6 months), based on similar numbers from ground-based radar experiments [2].

Though there are large uncertainties in the estimates of meteoroid flux in currently available models, particularly in the lower mass regimes, existing models provide an estimate of the number of impacts on ISOLDE during the course of its experiment duration. These estimates are shown in Fig. 11 for both picogram (10^{-12} g) shower meteoroids (left panel) using the Cour-Palais model [23], and the sporadic meteoroids (right panel) using the Grun model [24] which also contains the modeled (MASTERS) flux of orbital debris particles for comparison. Note that current debris models do not have the capability to predict the flux at masses lower than 1 pg.

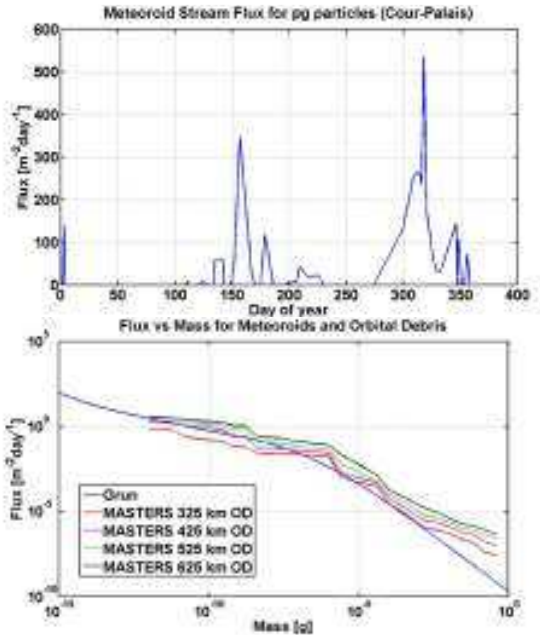

Figure 11. (top) Daily variation of picogram shower meteoroids (Cour-Palais model); (bottom) Sporadic meteoroid (Grun model) and orbital debris (MASTERS model) flux as a function of mass.

In the figures above, the response was generated by averaging over all directions. Given specific knowledge of the instrument payload location on ISS, the instrument orientation and impact panel angle would be optimized to maximize the expected impact rate.

Using both the effective meteoroid impact area on the impact panels (0.16 m^2) and the minimum meteoroid mass detectable by our ground-based sensors at MPIK (10^{-15} g), the number of detectable impacts on ISOLDE is determined. Estimates for a sun synchronous dawn-dusk orbit predict that we would detect approximately 175 sporadic meteoroids per day with mass greater than 10^{-15} g, and 6 sporadic meteoroids with mass greater than 10^{-12} g, which far exceeds the minimum number of impacts for mission success. This estimate assumes a zenith-oriented instrument package, which allows for impacts from multiple sources of sporadic meteoroids. In addition to obtaining impacts from sporadic meteoroids, an additional 50 impacts per day with mass greater than 10^{-12} g is likely during peak meteor showers.

Though the orbital debris flux varies significantly with altitude, an extrapolation of the orbital debris curve to the femtogram size range, results in 20

orbital debris impacts per day (accounting for the much slower speed (7-10 km/s)). Although orbital debris characterization is not one of the major science objectives of this mission, these impacts are distinguished from meteoroids using both speed and composition. The data from orbital debris impacts will be retained and made publicly available.

2 Relevance to Space Weather

For decades, meteoroids have been observed to play a significant role in the Earth's orbital environment and upper atmosphere. The continuous bombardment of the Earth by these small particles provides the dominant source of metallic atoms (e.g. Si, Na, Fe, K, and Ca) in the mesosphere and lower thermosphere (MLT) [25] and is responsible for a variety of phenomena in the atmosphere including sporadic-E. The metallic atoms ablated from these meteoroids are the source of mesospheric metal layers between 70 and 140 km altitude [25]. In addition, these particles are believed to provide the source of ice nuclei, which is necessary for the formation of noctilucent and polar stratospheric clouds [26][27]. Meteoroid plasma (i.e. meteor) observations also provide a unique opportunity for the measurement of gravity wave momentum flux in the MLT [28] and the study of plasma dissipation in the evolution of meteor trails [29]. However, the measurement of the input flux of meteoroids into the atmosphere remains largely uncertain, since no single technique is currently able to measure the entire range of incoming particles.

As discussed herein, meteoroids travel fast enough to ionize upon impact, and therefore pose a risk of causing damage to satellites through an "electrical" mechanism, which remains poorly understood. This electrical mechanism, which scales strongly with velocity ($\sim v^{3.5}$), occurs even for the smallest, and therefore most numerous meteoroids. Two of the most well-known spacecraft lost due to electrical effects associated with meteoroid impact include Olympus in 1993 [30] and the Landsat 5 in 2009; both satellites lost gyro stability during the peak of the Perseid shower. Many other spacecraft failures, loosely attributed to "space weather", are likely also be due to meteoroid impacts, since the catalyst for electrical anomalies typically remains undetermined. Through this mission, we will gain an understanding of the plasma physics associated with meteoroid impacts that will not only lead to new understanding of meteoroid and meteoroid plasma phenomena, but the associated risk to spacecraft.

Development and Implementation

The ISOLDE modules will be developed in collaboration between Stanford University and the Jet Propulsion Laboratory in Pasadena, CA (JPL). The implementation will consist first of the development of a module prototype at Stanford in consultation with JPL, with the full sensor suite and data acquisition and analysis support. The prototype development will transition to and engineering model development, at Stanford as well, with again consultation from JPL. The engineering model will then be the basis of the flight unit(s), produced at JPL, with appropriate copies made. The flight unit(s) will be fabricated to conform to both spaceflight standards best practice, as well as standards that meet the requirements for application and deployment on the ISS.

3 References

1. Jones, J. and P. Brown (1993), Sporadic meteor radiant distributions-orbital survey results, *Monthly Notices of the Royal Astronomical Society*, *265*, 524.

2. Close, S., M. Oppenheim, S. Hunt, and A. Coster (2004), A technique for calculating meteor plasma density and meteoroid mass from radar head echo scattering, *Icarus*, *168*, 43–52, doi:10.1016/j.icarus.2003.11.018.

3. Ceplecha, Z., J. Borovicka, W. G. Elford, D. O. ReVelle, R. L. Hawkes, V. I. Porubcan, and M. Simek (1998), Meteor phenomena and bodies, *Space Science Reviews*, *84*(3), 327–471, doi:10.1023/A:1005069928850.

4. McBride, N., and J. A. M. McDonnell (1999), Meteoroid impacts on spacecraft: sporadics, streams, and the 1999 Leonids, *Planetary and Space Science*, *47*(8-9), 1005–1013.

5. Bertaux, J. L. and J. E. Blamont (1976), Possible evidence for penetration of interstellar dust into the Solar System, *Nature*, *262*, 263–266.

6. Wolf, H., J. Rhee, and O. Berg (1976), Orbital elements of dust particles intercepted by Pioneers 8 and 9, in *Interplanetary Dust and Zodiacal Light*, *Lecture Notes in Physics*, vol. 48, edited by H. Elssser and H. Fechting, pp. 165–169, Springer Berlin / Heidelberg, doi:10.1007/3-540-07615-8_478.

7. Sasaki, S. et al. (2002) Observation of interplanetary and interstellar dust particles by Mars Dust Counter (MDC) on board NOZOMI, *Adv. Space Res.*, *29*(8), 1145–1153.

8. Harilal, S. S., C. V. Bindhu, M. S. Tillack, F. Najmabadi, and A. C. Gaeris (2003), Internal structure and expansion dynamics of laser ablation plumes into ambient gases, *Journal of Applied Physics*, *93*, 2380.

9. Starks, M. J., D. L. Cooke, B. K. Dichter, L. C. Chhabildas, W. D. Reinhart, and T. F. Thornhill III (2006), Seeking radio emissions from hypervelocity micrometeoroid impacts: Early experimental results

from the ground, *International Journal of Impact Engineering*, *33* (1-12), 781–787.

10. Burchell, M. J., L. Kay, and P. R. Ratcliff (1996), Use of combined light flash and plasma measurements to study hypervelocity impact processes, *Advances in Space Research*, *17*(12), 141–145.

11. Takano, T., Y. Murotani, K. Maki, T. Toda, A. Fujiwara, S. Hasegawa, A. Yamori, and H. Yano (2002), Microwave emission due to hypervelocity impacts and its correlation with mechanical destruction, *Journal of Applied Physics*, *92*, 5550.

12. Crawford, D., and P. Schultz (1999), Electromagnetic properties of impact-generated plasma, vapor and debris, *International Journal of Impact Engineering*, *23*(1), 169–180.

13. Crawford, D. A., and P. H. Schultz (1993), The production and evolution of impact-generated magnetic fields, *International Journal of Impact Engineering*, *14*(1-4), 205–216.

14. Close, S., P. Colestock, L. Cox, M. Kelley, and N. Lee (2010), Electromagnetic pulses generated by meteoroid impacts on spacecraft, *Journal of Geophysical Research*, *115*, A12328, doi:10.1029/2010JA015921.

15. Fletcher, A., (2013), Ph.D. Dissertation (in progress).

16. Lee, N., S. Close, D. Lauben, I. Linscott, A. Goel, T. Johnson, R. Srama, S. Bugiel, and A. Mocker (2011), Study of hypervelocity impact plasma expansion, in *3rd AIAA Atmospheric Space Environments Conference*, AIAA, Honolulu, HI.

17. Lee, N., et al. (2012), Measurements of freely-expanding plasma from hypervelocity impacts, *International Journal of Impact Engineering*, *44*, 40–49, doi:10.1016/j.ijimpeng.2012.01.002.

18. Maki, K., T. Takano, A. Fujiwara, and A. Yamori (2004), Radio-wave emission due to hypervelocity impacts in relation to optical observation and projectile speed, *Advances in Space Research*, *34*(5), 1085–1089.

19. Johnson, T., I. Linscott, S. Close, D. Strauss, N. Lee, R. Adamo, A. Mocker, R. Srama, and S. Bugiel (2011), Detection and analysis of RF data from hypervelocity impacts, *Proc. 3rd AIAA Atmos. Space. Env.*.

20. Eichhorn, G. (1975), Measurements of the light flash produced by high velocity particle impact, *Planetary and Space Science*, *23*(11), 1519–1525.

21. Enloe, C. L, L. Habash Krause, R. K. Haaland, T. T. Patterson, C. E. Richardson, C. C. Lazidis, and R. G. Whiting (2003), Miniaturized electrostatic analyzer manufactured using photolithographic etching, *Review of Scientific Instruments*, *74*, 1192–1195.

22. Enloe, C. L, L. Habash Krause, M. G. McHarg, and O. Nava (2004), Characterization of a plasma source for ground-based simulation of LEO plasma conditions, AIAA-2004-5668, *2nd International Energy Conversion Engineering Conference*, Providence, Rhode Island.

23. Cour-Palais, B. (1969), Meteoroid Environment Model – 1969, NASA SP-8013..

24. Grun, E., H. A. Zook, H. Fechtig, and R. H. Giese (1985), Collisional balance of the meteoritic complex, *Icarus*, *62*, 244–272.

25. Plane, J. M. C. (2003), Atmospheric chemistry of meteoric metals, *Chemical Reviews – Columbus*, *103*(12), 4963–4984.

26. Curtius, J., et al. (2005), Observations of meteoritic material and implications for aerosol nu- cleation in the winter Arctic lower stratosphere derived from in situ particle measurements, *Atmospheric Chemistry and Physics Discussions*, *5*(4), 5039–508

27. Megner, L., M. Rapp, and J. Gumbel (2006), Distribution of meteoric smoke–sensitivity to microphysical properties and atmospheric conditions, *Atmos. Chem. Phys.*, *6*, 4415–4426.

28. Fritts, D. C. et al. (2010), Southern Argentina Agile Meteor Radar: System design and initial measurements of large-scale winds and tides, *Journal of Geophysical Research*, *115*, D18112, doi:10.1029/2010JD013850.

29. Dyrud, L. P., E. Kudeki, and M. Oppenheim (2007), Modeling long duration meteor trails, *Journal of Geophysical Research*, *112*, A12307, doi:10.1029/2007JA012692.

30. Caswell, R. D., N. McBride, and A. Taylor (1995), Olympus end of life anomaly – a Perseid meteoroid impact event?, *International Journal of Impact Engineering*, *17*(1-3), 139–150, doi:10.1016/0734-743X(95)99843-G.